Journal of Sound and Vibration xxx (xxxx) xxx

Contents lists available at ScienceDirect

Journal of Sound and Vibration

journal homepage: www.elsevier.com/locate/jsv

Finite element model updating using in-situ experimental data

J.W.R. Meggitt*, A.T. Moorhouse

Acoustics Research Centre, University of Salford, Greater Manchester, M5 4WT United Kingdom

ARTICLE INFO

Article history:
Received 23 May 2020
Revised 30 July 2020
Accepted 27 August 2020
Available online xxx

Keywords:
Model updating
Sub-structure
In-situ measurement
Dynamic stiffness
Transmissibility
Invariants

ABSTRACT

Conventional model updating methods are based on frequency response function (FRF) and/or modal parameter estimates obtained from freely suspended, or sometimes rigidly constrained, sub-structures. These idealised boundary conditions are, however, often difficult to realise in a practical scenario. Furthermore, they are in conflict with the requirement that the sub-structure should also be measured whilst under a representative mounting condition. This paper addresses the question whether model updating can be achieved in the presence of an arbitrary or unknown boundary condition using in-situ measurements, i.e. without removing the sub-structure from its assembly. It is shown that some measurable properties, dynamic transfer stiffness and generalised transmissibility, are invariant to sub-structural boundary conditions and can therefore be obtained in-situ. It is further shown that, with minor adaption, existing transmissibility-based updating methods can be applied more widely than previously thought; to sub-structures whose boundary conditions are non-ideal. The theory is verified by a numerical beam example. Application to a resilient isolator is then demonstrated where a finite element model is successfully updated without removing the isolator from its assembly.

1. Introduction

Model updating describes a class of methods that use experimental data to identify the uncertain parameters of a numerical model [1,2]. Its primary purpose is to improve test-model correlation, i.e. the ability of a model to correctly represent the dynamics of a target structure. The numerical modelling of dynamic structures by means of Finite Element (FE), Boundary Element (BE), or analytical methods is common place, both in academic and industrial sectors. Often these models are used to assess structural integrity and operational survivability. This particular application requires a high degree of confidence in the model's outputs. For this reason experimental data is used to fine-tune model parameters until a sufficient degree of test-model correlation is achieved.

Existing methods for model updating can be broadly categorised by the type of experimental data that is used to quantify model correctness. Common choices include modal parameter estimates (natural frequencies and mode shapes) [1–3] and measured frequency response functions (FRFs) [4–8]. Together, measured and modelled data is used to formulate an objective function (representing test-model error) which is minimised by an appropriate optimisation algorithm. A typical objective function would be the mean squared error between measured and modelled natural frequencies, for example.

* Corresponding author.
E-mail address: j.w.r.meggitt1@salford.ac.uk (J.W.R. Meggitt).

https://doi.org/10.1016/j.jsv.2020.115675
0022-460X/

Whilst modal parameter based optimisation methods have seen greater attention in the literature, the advantages of FRF based methods are many, including; 1) errors in modal parameter estimates are avoided (these estimates can be challenging in the presence of highly damped/modal systems) and, 2) statistical solutions can be sought by considering an over-determined system of equations, this is made possible by the greater amount of information available from FRFs compared to modal parameter estimates. Furthermore, it has been shown that FRF anti-resonances contain the same information as mode shapes and natural frequencies together [9], yet are available by direct measurement.

Unfortunately for complex systems, FRF-based updating can involve large computational effort due to the use of full system matrices. Moreover, FRF sensitivities are non-monotonic functions of the updating parameters, meaning that their linearisation has limited validity. Other issues include the presence of noise, which can make convergence very slow and often numerically unstable [5,6], and the selection of which frequency points to use when updating [8]. What's more, in real-world structures it is often difficult to measure acting forces directly, complicating the measurement of their FRF matrices. This issue has led to an increased interest in output only methods for model updating.

In [10] Devriendt and Guillamue proposed an output only identification of modal parameters based on transmissibility measurements. In [11] Steenackers et al. proposed the use of transmissibility measurements to update FE models by identifying the natural frequencies of a constrained assembly. Meruane proposed an alternative approach where FRF anti-resonance frequencies are identified from output only transmissibility measurements [12].

To successfully update a numerical model based on experimental measurements, the acquired data, whether modal, FRF or transmissibility-based, should characterise the target sub-structure independently; they should be *invariant sub-structural properties*.[1] To ensure invariant sub-structure data is acquired, measurements must be performed with precisely known boundary conditions. This is most often achieved with the sub-structure uncoupled and suspended freely. Alternatively, a constrained interface boundary condition can be used, where the sub-structure's interface is rigidly constrained. Unfortunately, the above are in conflict with the requirement that the sub-structure should also be measured whilst under a representative mounting condition. Furthermore, achieving these idealised boundary conditions can often be challenging in a practical scenario. The above issues can be avoided, in part, by considering the unknown boundary conditions explicitly in the updating procedure; sub-structural properties are updated alongside the unknown boundary conditions. In this work we will consider an alternative approach, based on in-situ experimental testing.

In recent years several works have been devoted to the in-situ characterisation of sub-structures, i.e. the extraction of invariant sub-structural properties from measurements performed with the target sub-structure installed within an arbitrary assembly [13–15].[2] In the present paper we propose the application of *in-situ experimental testing*, and the extraction of invariant sub-structural properties, to update numerical sub-structure models. The key advantage of the proposed method is its potential to avoid the need to achieve an idealised boundary condition (i.e. free or constrained) when performing experimental tests for model updating purposes.

The remainder of this paper will be structured as follows. Section 2 will begin by introducing the invariant sub-structure quantities that are available from in-situ experimental testing, considering single and dual interface sub-structures. Section 3 will summarise the proposed in-situ updating strategy, and discuss the extension of previous works based on the developments herein. The proposed method will be demonstrated first by a numerical example in Section 4, and then by a simple experimental application in Section 5. Finally, some concluding remarks are made in Section 6.

2. In-situ sub-structure invariants

In this section we will introduce and derive the invariant sub-structure quantities that are available from in-situ experimental testing. These invariants will form the basis of the in-situ sub-structure model updating strategy proposed in Section 3.

We are interested in updating sub-structure models based on experimental data obtained from an assembly, i.e. with the target sub-structure subject to an unknown/arbitrary boundary condition. To do so we must determine an appropriate *invariant* sub-structure quantity from measurements available on the assembled structure. Depending on the nature of the sub-structure, i.e. whether it is a single or dual interface type (see Fig. 1), two suitable quantities are available; the dynamic stiffness [14,15] and the transmissibility [16]. The invariant nature of these quantities will be discussed in detail in this section.

The dynamic stiffness D_{ij} describes the relation between an applied displacement u_j at the DoF j, and the resulting force f_i at the DoF i, whilst all DoFs $k \neq j$ are subject to a rigid constraint,

$$\begin{pmatrix} f_1 \\ \vdots \\ f_N \end{pmatrix} = \begin{bmatrix} D_{11} & \cdots & D_{1N} \\ \vdots & \ddots & \vdots \\ D_{N1} & \cdots & D_{NN} \end{bmatrix} \begin{pmatrix} u_1 \\ \vdots \\ u_N \end{pmatrix}, \qquad D_{ij} = \left. \frac{f_i}{u_j} \right|_{u_{k\neq j}=0}. \tag{1}$$

Note that for $i \neq j$ the resultant force $f_i = \bar{f}_i$ is the blocking force necessary to constrain the DoF i such that $u_i = 0$.

[1] It should be noted that here we consider sub-structural invariance with respect to their connection to other sub-structures.
[2] This '*in-situ*' condition may equivalently be thought of as an unknown boundary condition on the target sub-structure.

Please cite this article as: J.W.R. Meggitt and A.T. Moorhouse, Finite element model updating using in-situ experimental data, Journal of Sound and Vibration, https://doi.org/10.1016/j.jsv.2020.115675

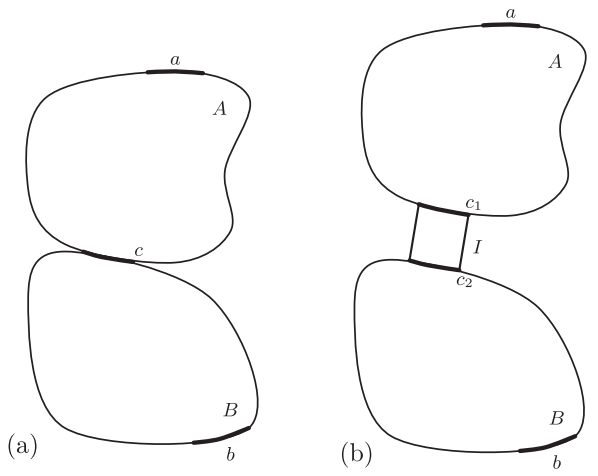

Fig. 1. Schematic representation of general single (a) and dual (b) interface assemblies.

Generally speaking, a transmissibility describes the relation between two like quantities. Common transmissibilities are those of force and displacement. The force transmissibility T^f_{ij} is defined here as the relation between an applied force f_j at the DoF j, and the blocking force $-\bar{f}_i$ at the DoF i, whilst all other (excitation) DoFs are subject to a zero force constraint $f_{k\neq j} = 0$,

$$\begin{pmatrix} -\bar{f}_1 \\ \vdots \\ -\bar{f}_N \end{pmatrix} = \begin{bmatrix} T^f_{11} & \cdots & T^f_{1M} \\ \vdots & \ddots & \vdots \\ T^f_{N1} & \cdots & T^f_{NM} \end{bmatrix} \begin{pmatrix} f_1 \\ \vdots \\ f_M \end{pmatrix}, \qquad T^f_{ij} = \left.\frac{-\bar{f}_i}{f_j}\right|_{f_{k\neq j}=0}. \tag{2}$$

Note that the excitation and blocking force DoFs belong to different sets ($j \in M$ and $i \in N$), and that if several blocking DoFs are considered, a constraint is applied to all, $u_{i\in N} = 0$.

The displacement transmissibility T^d_{ij} describes the relation between the displacement u_j at DoF j, and the displacement u_i at DoF i, due to the applied force f_k, whilst all other DoFs ($j \in N$) are subject to a rigid constraint,

$$\begin{pmatrix} u_1 \\ \vdots \\ u_M \end{pmatrix} = \begin{bmatrix} T^d_{11} & \cdots & T^d_{1N} \\ \vdots & \ddots & \vdots \\ T^d_{M1} & \cdots & T^d_{MN} \end{bmatrix} \begin{pmatrix} u_1 \\ \vdots \\ u_N \end{pmatrix}, \qquad T^d_{ij} = \left.\frac{u_i}{u_j}\right|_{u_{k\neq j}=0}. \tag{3}$$

Again, the two displacement DoFs belong to different sets ($j \in N$ and $i \in M$).

Note that there is a symmetry between the force and displacement transmissibility. Defined in terms of a blocking force, implicit to the force transmissibility are a set of rigid constraints. Similarly, by definition the displacement transmissibility requires the rigid constraint of all DoFs $k \neq j$. It has been shown that for multi-DoF structures the force and displacement based transmissibility are related through simple matrix manipulations [17].

The invariant nature of the above quantities arises due to the blocking constraints present in their definitions. If the blocking constraints are applied to the DoFs that separate the target sub-structure from the remainder of its assembly, the dynamics of neighbouring sub-structures are unable to influence the above quantities, and so they become invariant sub-structural properties. For brevity, invariant sub-structural properties will be referred to as 'invariants' hereafter.

In what follows, the above invariants will be derived for multi-DoF structures, and their invariance shown explicitly.

2.1. Single interface sub-structures

Let us begin by considering the coupled AB assembly in Fig. 1a. Two sets of DoFs are considered; the remote set a, located internal to sub-structure A, and the interface set c. The equations of motion that govern the coupled AB assembly are then,

$$\begin{pmatrix} \mathbf{f}_a \\ \mathbf{f}_c \end{pmatrix} = \begin{bmatrix} \mathbf{D}_{Aaa} & \mathbf{D}_{Aac} \\ \mathbf{D}_{Aca} & \mathbf{D}_{Acc} + \mathbf{D}_{Bcc} \end{bmatrix} \begin{pmatrix} \mathbf{u}_a \\ \mathbf{u}_c \end{pmatrix} \tag{4}$$

where $\mathbf{D}_{Nij}$ is a sub-structure (dynamic) stiffness matrix; where capitalised subscripts denote the sub-structure to which the sub-matrix belongs, and lowercase subscripts the DoFs between which it is defined. Note that the interface stiffness matrix is represented here by the summed interface stiffness matrices of sub-structures A and B, $\mathbf{D}_{ABcc} = \mathbf{D}_{Acc} + \mathbf{D}_{Bcc}$.

Please cite this article as: J.W.R. Meggitt and A.T. Moorhouse, Finite element model updating using in-situ experimental data, Journal of Sound and Vibration, https://doi.org/10.1016/j.jsv.2020.115675

From Eq. (4) it is clear that the remaining point and transfer stiffness matrices, $\mathbf{D}_{Aaa}$ and $\mathbf{D}_{Aac} = \mathbf{D}_{Aca}^{\mathrm{T}}$, are invariant properties of sub-structure A. Their direct measurement is, however, not generally practicable due to the need to constrain all DoFs bar the one under excitation (as per Eq. (1)). However, an alternative indirect approach is available. The coupled stiffness matrix $\mathbf{D}_{AB}$ is related by matrix inversion to the coupled reacceptance matrix $\mathbf{Y}_{AB}$,

$$\begin{bmatrix} \mathbf{D}_{Aaa} & \mathbf{D}_{Aac} \\ \mathbf{D}_{Aca} & \mathbf{D}_{Acc} + \mathbf{D}_{Bcc} \end{bmatrix} = \begin{bmatrix} \mathbf{Y}_{ABaa} & \mathbf{Y}_{ABac} \\ \mathbf{Y}_{ABca} & \mathbf{Y}_{ABcc} \end{bmatrix}^{-1}. \tag{5}$$

The receptance matrix of a structure is a readily measurable quantity.[3] The sub-structure invariants $\mathbf{D}_{Aaa}$ and $\mathbf{D}_{Aac} = \mathbf{D}_{Aca}^{\mathrm{T}}$ are therefore available experimentally from measurements with sub-structure A coupled to an arbitrary sub-structure B.

Conceptually, the inversion of measured receptance matrix has the effect of rigidly constraining all DoFs bar the one pertaining to the 'applied excitation', as per Eq. (1). Note that to successfully determine the invariants $\mathbf{D}_{Aaa}$ and $\mathbf{D}_{Aac} = \mathbf{D}_{Aca}^{\mathrm{T}}$ by matrix inversion it is essential that the description of interface c is sufficiently complete [18]; all *important* DoFs must be included in the measurement of $\mathbf{Y}_{AB}$. If an incomplete interface description is used the separating interface c will not be sufficiently constrained when the inversion is performed, and the dynamics of sub-structure B will manifest as errors on the acquired invariants. The appropriateness of an interface description can be assessed using the Interface Completeness Criterion as described in [18,19].

Based on Eq. (4) it is possible to formulate a third invariant as follows. By applying an appropriate blocking force at the interface c, we are able to enforce the constraint $\mathbf{u}_c = \mathbf{0}$ (and consequently $\mathbf{u}_b = \mathbf{0}$),

$$\begin{pmatrix} \mathbf{f}_a \\ -\bar{\mathbf{f}}_{Ac} \end{pmatrix} = \begin{bmatrix} \mathbf{D}_{Aaa} & \mathbf{D}_{Aac} \\ \mathbf{D}_{Aca} & \mathbf{D}_{Acc} + \mathbf{D}_{Bcc} \end{bmatrix} \begin{pmatrix} \mathbf{u}_a \\ \mathbf{0} \end{pmatrix}. \tag{6}$$

Note that this blocking force effectively removes the influence of sub-structure B from any quantities derived henceforth. From the top row of Eq. (6) we obtain,

$$\mathbf{u}_a = \mathbf{D}_{Aaa}^{-1}\mathbf{f}_a \tag{7}$$

which upon substitution into the second row yields,

$$-\bar{\mathbf{f}}_{Ac} = \mathbf{D}_{Aca}\mathbf{D}_{Aaa}^{-1}\mathbf{f}_a. \tag{8}$$

The matrix product in Eq. (8) may be interpreted as a generalised blocked force transmissibility. It relates an applied force $\mathbf{f}_a$ at the internal DoFs a, to the blocked force necessary to constrain the interface DoFs c. Let us define the blocked force transmissibility as,

$$\mathbf{T}_{Aca}^{f} = \mathbf{D}_{Aca}\mathbf{D}_{Aaa}^{-1} \tag{9}$$

such that,

$$-\bar{\mathbf{f}}_{Ac} = \mathbf{T}_{Aca}^{f}\mathbf{f}_a. \tag{10}$$

Noting that the transmissibility is defined as the product of two invariants, it is clearly also an invariant sub-structure property, thus we give it the capitalised sub-script A.

As discussed above, stiffness matrices are not directly available by measurement. It is therefore convenient to derive the blocked force transmissibility in terms of coupled receptances instead. According to the equivalent field theorem [13,20], a displacement field along the interface c, generated by an external force $\mathbf{f}_a$, can be reproduced identically by applying the (negative) blocking force $-\bar{\mathbf{f}}_{Ac}$ in place of the original excitation. We thus have the following equality,

$$\mathbf{u}_c = \mathbf{Y}_{Cca}\mathbf{f}_a = -\mathbf{Y}_{Ccc}\bar{\mathbf{f}}_{Ac} \tag{11}$$

where $\mathbf{Y}_{Cca}$ is the transfer repectance matrix of the coupled assembly from the internal DoFs a to the coupling interface c, and $\mathbf{Y}_{Ccc}$ is the point repectance matrix of the coupled assembly at the interface c.

Pre-multiplying both sides of Eq. (11) by the inverse receptance matrix $\mathbf{Y}_{Ccc}^{-1}$ then yields,

$$-\bar{\mathbf{f}}_{Ac} = \mathbf{Y}_{Ccc}^{-1}\mathbf{Y}_{Cca}\mathbf{f}_a. \tag{12}$$

Like Eq. (8), Eq. (12) relates the applied force $\mathbf{f}_a$ to the blocking force $-\bar{\mathbf{f}}_{Ac}$. We can then identify the blocked force transmissibility as,

$$\mathbf{T}_{Aca}^{f} = \mathbf{Y}_{Ccc}^{-1}\mathbf{Y}_{Cca} = \mathbf{D}_{Aca}\mathbf{D}_{Aaa}^{-1}. \tag{13}$$

It is significant that the above definition of force transmissibility is based entirely on *coupled* assembly receptances. The force transmissibility $\mathbf{T}_{Aca}^{f}$ is therefore a sub-structure invariant available from in-situ experimental testing.

With reference to Eq. (6), the blocked force transmissibility considered above can be interpreted as the relation between forces $\mathbf{f}_a$ and $-\bar{\mathbf{f}}_{Ac}$, due to the applied displacement $\mathbf{u}_a$. We can similarly consider a displacement transmissibility due to

[3] In practice it is more convenient to measure accelerance matrices (acceleration over force) and determine the receptance by assuming linearity and integrating twice with respect to time.

Please cite this article as: J.W.R. Meggitt and A.T. Moorhouse, Finite element model updating using in-situ experimental data, Journal of Sound and Vibration, https://doi.org/10.1016/j.jsv.2020.115675

an applied force. Consider the application of an external force at the interface c. The displacement response at the interface and internal DoFs are given, respectively, by

$$\mathbf{u}_c = \mathbf{Y}_{Ccc}\mathbf{f}_c \tag{14}$$

and

$$\mathbf{u}_a = \mathbf{Y}_{Cac}\mathbf{f}_c. \tag{15}$$

Note that the displacements $\mathbf{u}_c$ and $\mathbf{u}_a$ are responses to the same excitation. Rearranging Eq. (15) to determine $\mathbf{f}_c$ and substituting this into Eq. (14) leads to the displacement transmissibility relation,

$$\mathbf{u}_c = \mathbf{Y}_{Ccc}\mathbf{Y}_{Cac}^{-1}\mathbf{u}_a = \mathbf{T}_{Aca}^{d}\mathbf{u}_a \tag{16}$$

where,

$$\mathbf{T}_{Aca}^{d} = \mathbf{Y}_{Ccc}\mathbf{Y}_{Cac}^{-1}. \tag{17}$$

At first sight it is not obvious that the displacement transmissibility is also a sub-structure invariant. This is made clearer by considering the nature of the external force $\mathbf{f}_c$. Note that the dynamic influence of sub-structure B onto A (i.e. due to internal coupling forces) can be represented by an appropriate external force $\mathbf{f}_c$, and that no requirements were placed on the nature of this external force in deriving Eq. (16). Hence, Eq. (16) is valid in the presence of an arbitrary forcing term, and so the displacement transmissibility $\mathbf{T}_{Aca}^{d}$ is an invariant sub-structural property.

From inspection of Eq. (13) and 17, it is clear that the force and displacement transmissibilities are related. Recalling Eqs. (13) and (17),

$$\mathbf{T}_{Aca}^{f} = \mathbf{Y}_{Ccc}^{-1}\mathbf{Y}_{Cca} \tag{18}$$

$$\mathbf{T}_{Aca}^{d} = \mathbf{Y}_{Ccc}\mathbf{Y}_{Cac}^{-1}. \tag{19}$$

we can see that,

$$\mathbf{T}_{Aca}^{f} = \mathbf{Y}_{Ccc}^{-1}\mathbf{Y}_{Cca} = \left(\mathbf{Y}_{Ccc}\mathbf{Y}_{Cac}^{-1}\right)^{-\mathrm{T}} = \left(\mathbf{T}_{Aca}^{d}\right)^{-\mathrm{T}}. \tag{20}$$

The force transmissibility is equal to the inverse of the transposed displacement transmissibility [17], both of which are invariant sub-structural properties. For a more detailed discussion regarding force and displacement-based transmissibilities and their applications the reader is referred to the following works [10,16,17,21,22].

In the above, both force and displacement transmissibilities were defined in terms of coupled assembly receptances. Whilst these receptances are readily measurable quantities, requiring a known input force and measured displacement response (or more practically, an acceleration response), it would not be unreasonable to expect scenarios where such measurements are impractical, for example if access to the target sub-structure is restricted so that the necessary excitations cannot be applied. As an alternative to requiring receptance matrices, it is possible define the transmissibility in terms of output only quantities.

Suppose sub-structure A is installed within an active assembly, i.e. an assembly containing one or more vibration generating mechanisms. In this case it is possible to determine the transmissibility based on measurements of the operational displacement only. A key requirement of the above is that the vibration generating mechanisms do not reside within the target sub-structure, as the excitation DoFs (taken here to be those of the interface c) must be known.

To extend the definition of transmissibility to output only quantities it is sufficient to consider N linearly independent operational states of the assembly AB. From the perspective of sub-structure A, each operational state can be represented by an external force $\mathbf{f}_c^{(i)}$. Arranging each external force vector as the columns of a matrix we arrive at the external force matrix $\mathbf{F}_c = \left[\mathbf{f}_c^{(1)} \quad \cdots \quad \mathbf{f}_c^{(N)}\right]$. Eqs. (14) and (15) can thus be rewritten as,

$$\mathbf{U}_c = \mathbf{Y}_{Ccc}\mathbf{F}_c \tag{21}$$

and

$$\mathbf{U}_a = \mathbf{Y}_{Cac}\mathbf{F}_c \tag{22}$$

and Eq. (16) as,

$$\mathbf{U}_c = \mathbf{Y}_{Ccc}\mathbf{Y}_{Cac}^{-1}\mathbf{U}_a, \tag{23}$$

where $\mathbf{U}_c$ and $\mathbf{U}_a$ represent operational displacement response matrices at, respectively, the interface and internal DoFs of sub-structure A. From Eq. (23) it is straightforward to identify the displacement transmissibility matrix,

$$\mathbf{T}_{Aca}^{d} = \mathbf{Y}_{Ccc}\mathbf{Y}_{Cac}^{-1} = \mathbf{U}_c\mathbf{U}_a^{-1}. \tag{24}$$

Similarly, using Eq. (20) we can define the force transmissibility matrix as,

$$\mathbf{T}_{Aca}^{f} = \left(\mathbf{U}_c\mathbf{U}_a^{-1}\right)^{-\mathrm{T}} = \mathbf{U}_c^{-\mathrm{T}}\mathbf{U}_a^{\mathrm{T}}. \tag{25}$$

Please cite this article as: J.W.R. Meggitt and A.T. Moorhouse, Finite element model updating using in-situ experimental data, Journal of Sound and Vibration, https://doi.org/10.1016/j.jsv.2020.115675

Eqs. (24) and (25) provide output only definitions of the sub-structure invariants $\mathbf{T}^d_{Aca}$ and $\mathbf{T}^f_{Aca}$, respectively, requiring measurement of operational displacements only. Note however, that to determine the transmissibility by means of output only measurements, as per Eqs. (24) and (25), the inverted displacement response matrix must be of full rank; each operational state must produce a linearly independent displacement response. For more details on this application of Eq. (24) the reader is referred to [16].

In summary of this section, we have shown that the dynamic stiffness elements, $\mathbf{D}_{Aaa}$ and $\mathbf{D}_{Aac} = \mathbf{D}^{\mathrm{T}}_{Aca}$, the force transmissibility $\mathbf{T}^f_{Aca}$, and the displacement transmissibility $\mathbf{T}^d_{Aca}$, are not only invariant sub-structural properties of A, but are all available from measurements conducted *in-situ*, i.e. with an arbitrary boundary condition at c. Furthermore, the transmissibilities may in principle be obtained from output only measurements.

Note that an equivalent set of invariants can be defined for sub-structure B by simply replacing all sub-script indices a with b, and A with B. Similarly, by considering both sub-structures A and B simultaneously Eq. (5) can be extended as so,

$$\begin{bmatrix} \mathbf{D}_{Aaa} & \mathbf{D}_{Aac} & \mathbf{0} \\ \mathbf{D}_{Aca} & \mathbf{D}_{Acc} + \mathbf{D}_{Bcc} & \mathbf{D}_{Bcb} \\ \mathbf{0} & \mathbf{D}_{Bbc} & \mathbf{D}_{Bbb} \end{bmatrix} = \begin{bmatrix} \mathbf{Y}_{ABaa} & \mathbf{Y}_{ABac} & \mathbf{Y}_{ABab} \\ \mathbf{Y}_{ABca} & \mathbf{Y}_{ABcc} & \mathbf{Y}_{ABcb} \\ \mathbf{Y}_{ABba} & \mathbf{Y}_{ABbc} & \mathbf{Y}_{ABbb} \end{bmatrix}^{-1}. \tag{26}$$

If the DoFs a, b and c are all included in the measurement of $\mathbf{Y}_{AB}$, the invariants of both sub-structure A and B are available. The above arguments can clearly be extended to include additional sub-structures C, D, $\cdots$, etc.

2.2. Dual interface sub-structures (coupling elements)

In Section 2.1 we considered the invariants of single interface sub-structures, i.e. those where we are able to group all interface DoFs into the single set c, whilst defining a second set of internal DoFs a. Often when dealing with coupling elements (see Fig. 1b), such as vibration isolators, it is not possible to define a (measurable) set of internal DoFs. This limits the invariants available from in-situ testing.

With reference to Fig. 1b, if access to some set of internal DoFs on the coupling element is possible, it may be treated as a single interface sub-strucutre by simply grouping together the interface DoFs c_1 and c_2 to form the DoF set c. We then have access to both stiffness and transmissibility-based invariants, as per Section 2.1. If access is available only to the interface DoFs c_1 and c_2, the only available invariant is the transfer stiffness $\mathbf{D}_{Ic_1c_2} = \mathbf{D}^{\mathrm{T}}_{Ic_2c_1}$.

Like the AB assembly considered before, the stiffness matrix of the AIB assembly is available through the inversion of a measured assembly receptance matrix,

$$\begin{bmatrix} \mathbf{D}_{Ac_1c_1} + \mathbf{D}_{Ic_1c_1} & \mathbf{D}_{Ic_1c_2} \\ \mathbf{D}_{Ic_2c_1} & \mathbf{D}_{Ic_2c_2} + \mathbf{D}_{Bc_2c_2} \end{bmatrix} = \begin{bmatrix} \mathbf{Y}_{AIBc_1c_1} & \mathbf{Y}_{AIBc_1c_2} \\ \mathbf{Y}_{AIBc_2c_1} & \mathbf{Y}_{AIBc_2c_2} \end{bmatrix}^{-1}. \tag{27}$$

From Eq. (27) it is clear that the dynamic transfer stiffness $\mathbf{D}_{Ic_1c_2} = \mathbf{D}^{\mathrm{T}}_{Ic_2c_1}$ of the coupling element is available from in-situ experimental testing.

Eq. (27) has found several applications in the literature, including the independent characterisation of vibration isolators [15,23] and the in-situ decoupling of resiliently coupled sub-structures [24].

Like Eq. (5), successful implementation of Eq. (27) requires that all important interface DoFs are included in the measurement of $\mathbf{Y}_{AIB}$.

3. In-situ sub-structure model updating

In conventional model updating, experimental testing is performed on the uncoupled target sub-structure (say A), and its free interface receptance matrix $\mathbf{Y}_A$ is measured. The receptance $\mathbf{Y}_A$ is used either to update the numerical model directly, or to estimate modal parameters (natural frequencies and mode shapes) which are themselves used to update the numerical model. In this paper we propose an alternative approach, based on in-situ sub-structure invariants, thus avoiding the need to achieve an idealised boundary condition on the target sub-structure.

The proposed in-situ model updating strategy is illustrated in Fig. 2. A numerical model (labelled FE) of the target sub-structure (say A or I) is built and its invariants computed. The physical target sub-structure (labelled exp) is installed in an appropriate manner, measured, and its invariants computed. The numerical and experimental invariants are then used to formulate an appropriate cost function,

$$J_S(\theta) = J_S\left(\mathbf{T}^{f,FE}_{Sca}(\theta), \mathbf{D}^{FE}_{Sca}(\theta), \mathbf{D}^{FE}_{Saa}(\theta), \mathbf{T}^{f,exp}_{Sca}, \mathbf{D}^{exp}_{Sca}, \mathbf{D}^{exp}_{Saa}\right), \tag{28}$$

or for a dual interface sub-structure,

$$J_D(\theta) = J_D\left(\mathbf{D}^{FE}_{Ic_1c_2}(\theta), \mathbf{D}^{exp}_{Ic_1c_2}\right) \tag{29}$$

where $\boldsymbol{\theta}$ is the vector of numerical parameters to be updated. This cost function is then minimised using an appropriate optimisation algorithm.

It is noted that the primary aim of this paper is to propose and verify the application of *in-situ* experimental testing as a means of updating numerical *sub-structure* models. Some simple examples are given in the numerical and experimental

Please cite this article as: J.W.R. Meggitt and A.T. Moorhouse, Finite element model updating using in-situ experimental data, Journal of Sound and Vibration, https://doi.org/10.1016/j.jsv.2020.115675

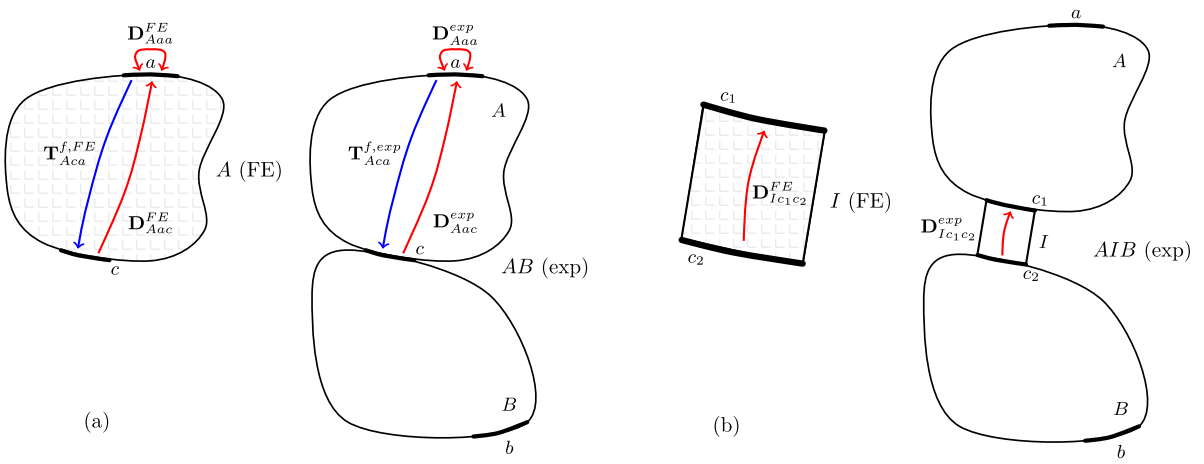

Fig. 2. In-situ sub-structure model updating. (a) - single interface sub-structure. (b) - dual interface sub-structure.

studies presented in Sections 4 and 5. However, a detailed investigation into the choice of cost function and the preferred optimisation algorithm is considered beyond the scope of this work, and the reader is referred to the many recognised publications e.g. [1,2] for further details. Nevertheless, by recognising related works in the literature, in particular other transmissibility-based approaches, alongside the notion of sub-structure invariants, ready to implement algorithms can be formulated.

In [11] and [12] two transmissibility-based approaches are presented for updating numerical models. Neither however, acknowledge the invariant nature of the transmissibility (when constraints are located at the interface) and therefore their potential to update numerical models using *in-situ* experimental data. A novel contribution of this paper is therefore to propose that, with simple modifications, these techniques can be applied more widely than originally envisaged, specifically to the *in-situ* updating of sub-structures.

In [11] Steenackers et al. proposed an updating procedure based on the measurement of transmissibility, as opposed to receptances or estimated modal parameters. Their key observation was that the peaks of a transmissibility curve correspond to the natural frequencies of a structure when the excitation DoF is rigidly constrained. The procedure was to experimentally determine the transmissibility between a series of *internal* DoFs on the target structure. In their example the target structure was rigidly clamped to a foundation, thus enforcing a known boundary condition. The authors then proposed the updating of a constrained FE model, based on the experimental transmissibility peaks. Once updated the model's constraints are removed and the procedure is complete. This transmissibility-based approach was posed as an output only solution to model updating, as the transmissibility can be determined from operational responses alone (see Eq. (25)).

Based on the developments of Section 2, the updating procedure presented in [11] can be extended to update *sub-structure* models[4] based on *in-situ* experimental measurements. All that is required is the relocation of the internal 'excitation' DoFs to the separating interface *c*. The peaks of the resulting transmissibility correspond to the natural frequencies of the (constrained) target sub-structure alone, as the unknown interface boundary condition has been replaced by a rigid constraint. The detailed procedure and cost function demonstrated in [11] can then be followed identically.

In [12] Meruane proposed an alternative transmissibility-based approach, instead using transmissibility measurements to identify FRF anti-resonance frequencies for model updating purposes. In [9] it was shown that anti-resonance sensitivities are a linear combination of eigenvalue and mode shape sensitivities, and so provide the same amount of information. Meruane proposed an algorithm capable of automatically identifying anti-resonance frequencies from measured transmissibility functions. Paired with the optimisation algorithm presented in [25], Meruane presented an output only transmissibility-based model updating procedure [12].

Like the constrained model optimisation proposed by Steenackers et al. [11], Meruane's anti-resonance-based approach can readily be extended to suit *in-situ* sub-structure model updating by again relocating the excitation DoFs to separating interface *c*.

The above transmissibility-based updating procedures may be adapted straightforwardly to suit an in-situ model updating, thus avoiding the need to achieve an idealised boundary condition across the target sub-structure's interface. Alternatively, more conventional FRF-based procedures can be adapted to suit the sub-structure invariants acquired (transmissibility and dynamics stiffness).

[4] Or whole structure models with unknown boundary conditions.

Please cite this article as: J.W.R. Meggitt and A.T. Moorhouse, Finite element model updating using in-situ experimental data, Journal of Sound and Vibration, https://doi.org/10.1016/j.jsv.2020.115675

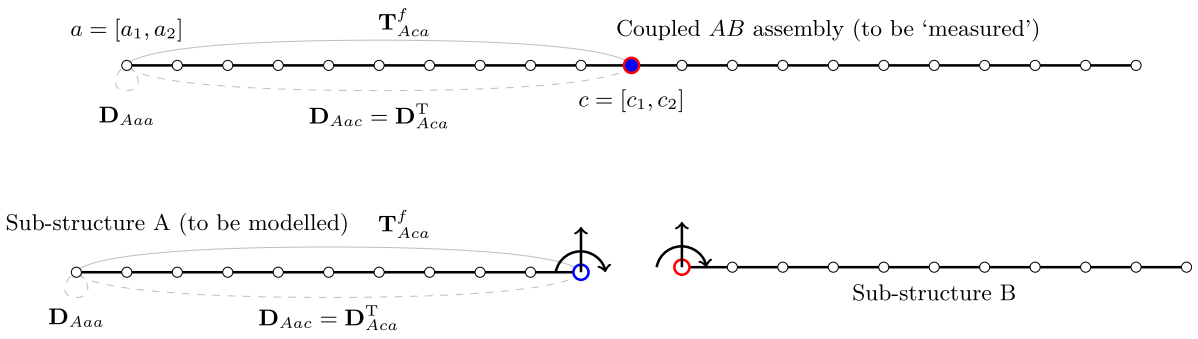

Fig. 3. Numerical model of single interface sub-structure.

3.1. Summary of in-situ updating strategy

In summary, the proposed strategy for updating a (single interface) sub-structure model using in-situ experimental testing may be outlined as follows:

1) Instrument the target sub-structure whilst *installed*, ensuring that all interface DoFs c are accounted for. If the dynamic transfer stiffness is also to be used the second set of internal DoFs a should also be instrumented.
2) Measure the coupled receptance matrices $\mathbf{Y}_{ABcc}$, $\mathbf{Y}_{ABac}$, $\mathbf{Y}_{ABca}$ and $\mathbf{Y}_{ABaa}$.
3) Build a numerical model of the *uncoupled* target sub-structure and choose the parameters $\boldsymbol{\theta}$ to be updated.
4) Calculate numerical and experimental sub-structure invariants.
5) Formulate an appropriate cost function $J(\boldsymbol{\theta})$ and update the model parameters accordingly.

For a dual interface sub-structure the same steps are followed but the interface DoFs c_1 and c_2 are considered.

Mathematically, model updating is an under-determined problem. Its success relies on acquiring a sufficient quantity of experimental data, from which the unknown model parameters can be determined. When considering a single interface sub-structure, the number of interface DoFs c is dictated by the structure. The number of remote DoFs a however, is arbitrary. Hence, many remote DoFs can be chosen to yield a sufficient amount of (invariant) experimental data. From a practical point of view, in the presence of a large number of remote DoFs the force transmissibility-based approach is likely more robust. The matrix inversion in Eq. (13) considers only the set of interface DoFs. Additional remote a DoFs can be included without worry of ill-conditioning the inversion. Furthermore, the transmissibility-based approach requires response measurements only at the interface; additional transmissibilities can be determined with minimal experimental effort (additional force excitations at a). In contrast, the stiffness-based method requires a response measurement at each a DoF considered (as well as the interface DoFs c). Although more expensive practically, together the point and transfer stiffness provide a greater amount of information than the transmissibility alone.

When considering a dual interface sub-structure, where the only invariant available is the transfer stiffness, the amount of experimental data available is limited by the number of interface DoFs present. For a typical coupling element, such as vibration isolator, the transfer stiffness alone may prove sufficient to update a model given the element's simple dynamics.

In the following section the above procedure will be demonstrated using a simple numerical example consisting of coupled beam structures. Following this, in Section 5, an experimental example will be shown where a simplified FE model of a vibration isolator is updated using in-situ experimental data.

4. Numerical example

In this section we will demonstrate the in-situ model updating procedure by means of two numerical examples. These examples are based on FE beam models and consider both single and dual interface sub-structures.

4.1. Single interface

Shown in Fig. 3 is a schematic representation of the example considered here. Two FE beams (A and B, each composed of 10 elements) are attached at their interface DoFs $c = [c_1, c_2]$ to form a coupled assembly. Material properties and sub-structure geometry are presented in Table 1.

This coupled assembly represents the 'test structure', on which (simulated) measurements are performed. Based on these simulated measurements the invariants of sub-structure A are determined, including the transmissibility $\mathbf{T}^f_{Aca}$, and the dynamic stiffness matrices $\mathbf{D}_{Aca}$ and $\mathbf{D}_{Aaa}$, where $a = [a_1, a_2]$ represents the two left most DoFs on sub-structure A (chosen arbitrarily). Note that each nodal point contains both translational (a_1, c_1) and rotational (a_2, c_2) DoFs. The invariants determined from the coupled assembly are then used to update the material properties of an FE model of sub-structure A alone (i.e. sub-structure B is not included in the updated model).

Please cite this article as: J.W.R. Meggitt and A.T. Moorhouse, Finite element model updating using in-situ experimental data, Journal of Sound and Vibration, https://doi.org/10.1016/j.jsv.2020.115675

Table 1
Sub-structural properties of test structures in Fig. 3 and 8.

Sub-structure	$L \times W \times H$ (m)	ρ (kg/m^3)	E (N/m^2)	η (-)
A (target, Section 4.1)	0.4 × 0.05 × 0.01	7000	2×10^9	0.05
B	0.4 × 0.03 × 0.01	7000	2×10^9	0.05
I (target, Section 4.2)	0.25 × 0.04 × 0.005	4000	2×10^7	0.05

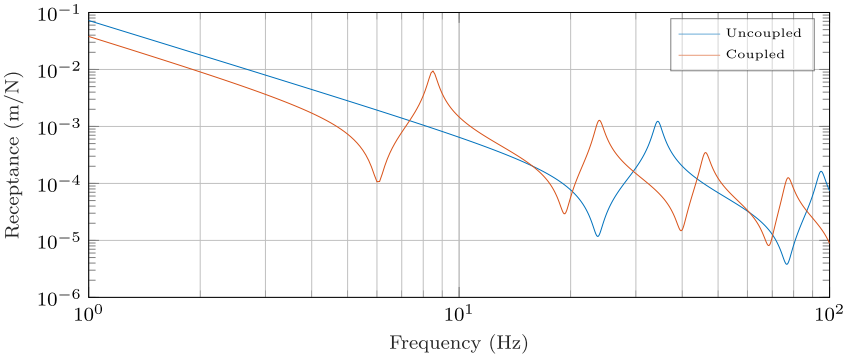

Fig. 4. Point receptances obtained from the coupled $Y_{ABa_1a_1}$ and uncoupled $Y_{Aa_1a_1}$ source sub-structure. (For interpretation of the references to colour in this figure legend, the reader is referred to the web version of this article.)

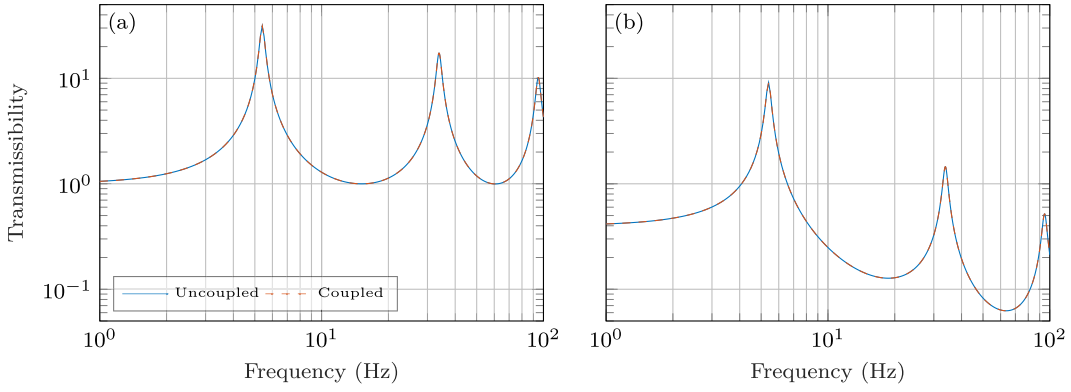

Fig. 5. Transmissibilities $T^f_{Ac_1a_1}$ (a) and $T^f_{Ac_2a_1}$ (b) obtained from the coupled and uncoupled source sub-structure.

To determine the sub-structure invariants the following calculations are performed on the assembled structure, as per Section 2. For the transmissibility,

$$\begin{bmatrix} T^f_{Ac_1a_1} & T^f_{Ac_1a_2} \\ T^f_{Ac_2a_1} & T^f_{Ac_2a_2} \end{bmatrix} = \begin{bmatrix} Y_{ABc_1c_1} & Y_{ABc_1c_2} \\ Y_{ABc_2c_1} & Y_{ABc_2c_2} \end{bmatrix}^{-1} \begin{bmatrix} Y_{ABc_1a_1} & Y_{ABc_1a_2} \\ Y_{ABc_2a_1} & Y_{ABc_2a_2} \end{bmatrix} \tag{30}$$

and for the dynamic stiffness,

$$\begin{bmatrix} D_{Aa_1a_1} & D_{Aa_1a_2} & D_{Aa_1c_1} & D_{Aa_1c_2} \\ D_{Aa_2a_1} & D_{Aa_2a_2} & D_{Aa_2c_1} & D_{Aa_2c_2} \\ D_{Ac_1a_1} & D_{Ac_1a_2} & D_{Ac_1c_1} + D_{Bc_1c_1} & D_{Ac_1c_2} + D_{Bc_1c_2} \\ D_{Ac_2a_1} & D_{Ac_2a_2} & D_{Ac_2c_1} + D_{Bc_2c_1} & D_{Ac_2c_2} + D_{Bc_2c_2} \end{bmatrix} = \begin{bmatrix} Y_{ABa_1a_1} & Y_{ABa_1a_2} & Y_{ABa_1c_1} & Y_{ABa_1c_2} \\ Y_{ABa_2a_1} & Y_{ABa_2a_2} & Y_{ABa_2c_1} & Y_{ABa_2c_2} \\ Y_{ABc_1a_1} & Y_{ABc_1a_2} & Y_{ABc_1c_1} & Y_{ABc_1c_2} \\ Y_{ABc_2a_1} & Y_{ABc_2a_2} & Y_{ABc_2c_1} & Y_{ABc_2c_2} \end{bmatrix}^{-1} \tag{31}$$

where AB denotes a measurement made on the coupled assembly.

Shown in Fig. 4 are the point receptances of sub-structure A when coupled ($\mathbf{Y}_{ABaa}$) and uncoupled ($\mathbf{Y}_{Aaa}$). Its clear from Fig. 4 that the attachment of sub-structure B influences greatly the dynamics of sub-structure A. This influence can be considered as the effect of an unknown boundary condition at c. In a typical model updating procedure sub-structure B must be removed to achieve an idealised (free) boundary condition at c. The in-situ model updating procedure avoids this, by instead extracting invariant sub-structure properties from the coupled assembly. Shown in Fig. 5 are the force transmissibilities $T^f_{Ac_1a_1}$ and $T^f_{Ac_2a_1}$ of sub-structure A based the coupled and uncoupled simulations. As expected the two are in exact agreement; this demonstrates the invariant nature of the force transmissibility when response DoFs are located at the sep-

Please cite this article as: J.W.R. Meggitt and A.T. Moorhouse, Finite element model updating using in-situ experimental data, Journal of Sound and Vibration, https://doi.org/10.1016/j.jsv.2020.115675

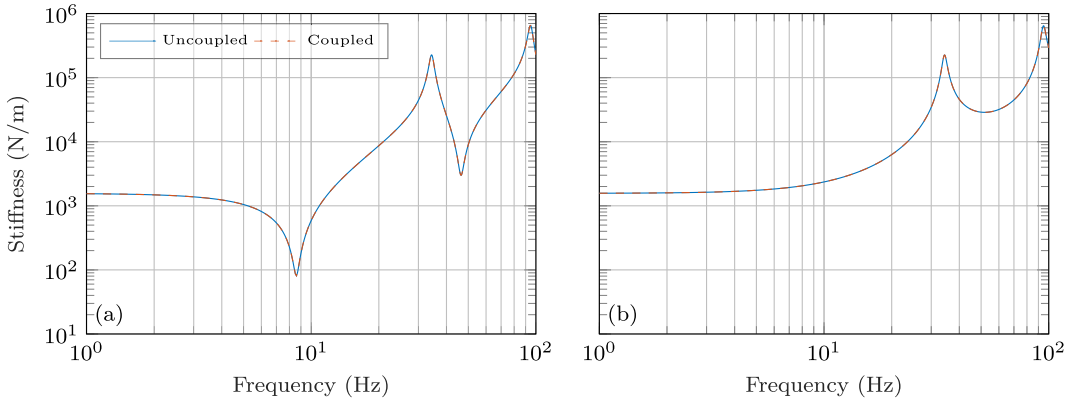

Fig. 6. Point and transfer dynamic stiffnesses $D_{Aa_1a_1}$ (a) and $D_{Aa_1c_1}$ (b) obtained from the coupled and uncoupled source sub-structure. Note that the coupled and uncoupled transfer stiffness curves are indistinguishable.

arating interface.[56] Note that, as per [11], the transmissibility peaks correspond to the natural frequencies of sub-structure A when its interface DoFs c (both translational and rotational) are constrained, i.e. with a clamped boundary condition. By calculating the transmissibility matrix $\mathbf{T}^f_{Aca}$ with all interface DoFs c present we enforce this idealised boundary condition mathematically, thus removing the unknown boundary condition representing the dynamics of sub-structure B.

Shown in Fig. 6 are the dynamic point and transfer stiffnesses $D_{Aa_1a_1}$ and $D_{Aa_1c_1}$ of sub-structure A based on the coupled and uncoupled simulations. As expected the two are in exact agreement; this demonstrates the invariant nature of the dynamic stiffness when all interface DoFs are included in the matrix inversion. As per the definition of dynamic stiffness, all DoFs, bar that of the excitation, are constrained. By including the interface DoFs c in the coupled receptance measurements, its inversion mathematically enforces a constrained interface boundary condition, thus removing the unknown boundary condition representing the dynamics of sub-structure B.

Figs. 5 and 6 demonstrate the invariance of the sub-structural properties $\mathbf{T}^f_{Aca}$, $\mathbf{D}_{Aac}$ and $\mathbf{D}_{Aaa}$. To update a numerical model of sub-structure A we formulate a cost function, using these invariants, which must be minimised with respect to the updating parameters $\boldsymbol{\theta}$.

The cost function chosen (out of many possible options) is,

$$J(\theta) = \sum^{n} \left\| \omega_n^{(T,FE)} - \omega_n^{(T,exp)} \right\|^2 + \sum^{\omega} \sum^{a} \left\| \mathbf{D}^{(FE)}_{Aaa}(\omega) - \mathbf{D}^{(exp)}_{Aaa}(\omega) \right\|^2 \tag{32}$$

where; $\omega_n^{(T,FE)}$ and $\omega_n^{(T,exp)}$ represent the frequency of the nth transmissibility peak for the uncoupled (to be updated) and coupled (test) models and, $\mathbf{D}^{(FE)}_{Aaa}(\omega)$ and $\mathbf{D}^{(exp)}_{Aaa}(\omega)$ are the point stiffness matrices for the uncoupled (to be updated) and coupled (test) models. The updating parameters are chosen to be the global material properties: density ρ, Young's modulus E and loss factor η.

Eq. (32) is minimised using a gradient based optimisation (*fmincon( )* in MATLAB). To avoid the issue of local minima, N random initialisations are drawn and the best performing (yielding the minimum $J(\theta)$) is chosen. To limit the search space, the updating parameters are limited by the following bounds, $3000 \leq \rho \leq 12000$, $10^4 \leq E \leq 10^{12}$ and $0.025 \leq \eta \leq 0.1$. It should be noted that a more robust cost function and optimisation algorithm may be necessary in a more practical scenario. The above example was chosen simply to verify the use of *in-situ* experimental testing for model updating.

Shown in Fig. 7 are the point receptences $Y_{Aa_1a_1}$ of the target and updated sub-structure model. Also shown is an example of an initial point receptance from which the updating procedure began. As expected given the numerical nature of this example, the updated sub-structure model is in agreement with the target sub-structure. Importantly, this updating procedure was based entirely on *coupled assembly simulations*, yet it was able to refine a model of sub-structure A alone.

4.2. Dual interface

In this section we will briefly consider the updating of a dual interface sub-structure. Dual interface sub-structures are commonplace in engineering structures, a typical example being vibration isolators, or other resilient couplings. Shown in Fig. 8 is a schematic representation of the example considered here. Three FE beams (*A, I* and *B*, each composed of 10 elements) are attached at their interface DoFs $c_1 = [c_{11}, c_{12}]$ and $c_2 = [c_{21}, c_{22}]$ to form a coupled assembly $C = AIB$. Material properties and sub-structure geometry are presented in Table 1. This coupled assembly represents the 'test structure', on

[5] Had the responses been located at some internal DoFs on A, the obtained transmissibility would not be invariant.

[6] Note that if the displacement transmissibility were considered, the excitation DoFs (as opposed to the response) would be located at the separating interface.

Please cite this article as: J.W.R. Meggitt and A.T. Moorhouse, Finite element model updating using in-situ experimental data, Journal of Sound and Vibration, https://doi.org/10.1016/j.jsv.2020.115675

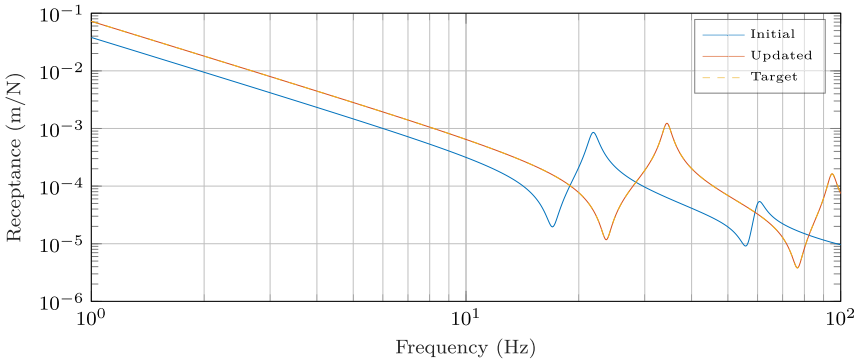

Fig. 7. Initial, updated and target point receptance $Y_{Aa_1a_1}$. Note that the updated and target curves are near indistinguishable.

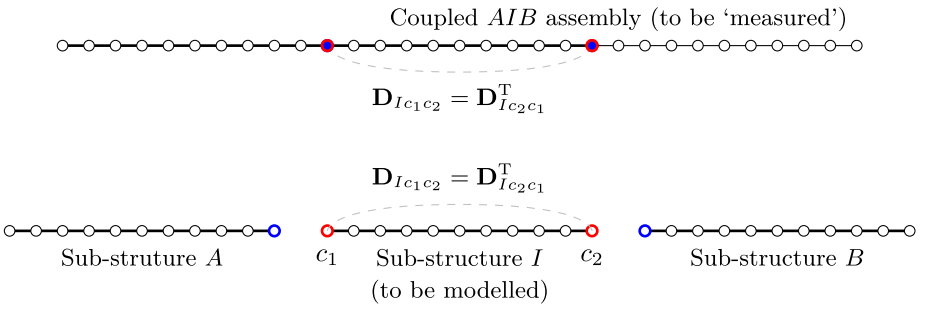

Fig. 8. Numerical model of dual interface sub-structure and coupled assembly.

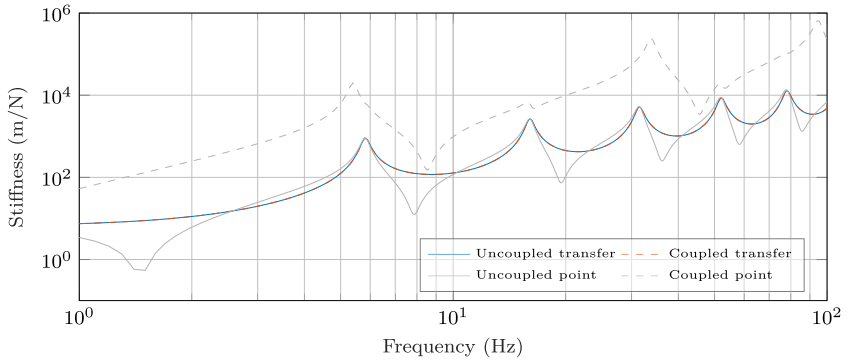

Fig. 9. Transfer stiffness $D_{Ic_{11}c_{21}}$ obtained from uncoupled and coupled sub-structure. Also shown in grey are the point stiffnesses $D_{Ic_{11}c_{11}}$ *and* $D_{AIc_{11}c_{11}}$.

which (simulated) measurements are performed. Based on these simulated measurements the invariants of sub-structure I are determined. If the only accessible DoFs are those of the interface (c_1 and c_2) the only invariant available is the dynamic transfer stiffness $\mathbf{D}_{Ic_1c_2} = \mathbf{D}^{\mathrm{T}}_{Ic_2c_1}$. If some set of internal DoFs a are also accessible, the interface DoFs can be grouped $c = [c_1, c_2]$, the sub-structure treated as a single interface type, and the additional invariants $\mathbf{T}^f_{Ica}$ and $\mathbf{D}_{Iaa}$ determined.

To determine the sub-structure invariants $\mathbf{D}_{Ic_1c_2} = \mathbf{D}^{\mathrm{T}}_{Ic_2c_1}$ the following calculations are performed on the assembled structure, as per Section 2,

$$\begin{bmatrix} D_{Ac_{11}c_{11}} + D_{Ic_{11}c_{11}} & D_{Ac_{11}c_{12}} + D_{Ic_{11}c_{12}} & D_{Ic_{11}c_{21}} & D_{Ic_{11}c_{22}} \\ D_{Ac_{12}c_{11}} + D_{Ic_{12}c_{11}} & D_{Ac_{12}c_{12}} + D_{Ic_{12}c_{12}} & D_{Ic_{12}c_{21}} & D_{Ic_{12}c_{22}} \\ D_{Ic_{21}c_{11}} & D_{Ic_{21}c_{12}} & D_{Ic_{21}c_{21}} + D_{Bc_{21}c_{21}} & D_{Ic_{21}c_{22}} + D_{Bc_{21}c_{22}} \\ D_{Ic_{22}c_{11}} & D_{Ic_{22}c_{12}} & D_{Ic_{22}c_{21}} + D_{Bc_{22}c_{21}} & D_{Ic_{22}c_{22}} + D_{Bc_{22}c_{22}} \end{bmatrix} = \begin{bmatrix} Y_{Cc_{11}c_{11}} & Y_{Cc_{11}c_{12}} & Y_{Cc_{11}c_{21}} & Y_{Cc_{11}c_{22}} \\ Y_{Cc_{12}c_{11}} & Y_{Cc_{12}c_{12}} & Y_{Cc_{12}c_{21}} & Y_{Cc_{12}c_{22}} \\ Y_{Cc_{21}c_{11}} & Y_{Cc_{21}c_{12}} & Y_{Cc_{21}c_{21}} & Y_{Cc_{21}c_{22}} \\ Y_{Cc_{22}c_{11}} & Y_{Cc_{22}c_{12}} & Y_{Cc_{22}c_{21}} & Y_{Cc_{22}c_{22}} \end{bmatrix}^{-1} \tag{33}$$

where C denotes a measurement made on the coupled assembly. Shown in Fig. 9 are the point and transfer stiffnesses obtained from the coupled ($D_{AIc_{11}c_{11}}$, $D_{Ic_{11}c_{21}}$) and uncoupled ($D_{Ic_{11}c_{11}}$, $D_{Ic_{11}c_{21}}$) sub-structure I. It is clear from Fig. 9 that the presence of sub-structures A and B have a considerable influence on the point stiffness of sub-structure I, whilst its transfer stiffness is invariant.

Please cite this article as: J.W.R. Meggitt and A.T. Moorhouse, Finite element model updating using in-situ experimental data, Journal of Sound and Vibration, https://doi.org/10.1016/j.jsv.2020.115675

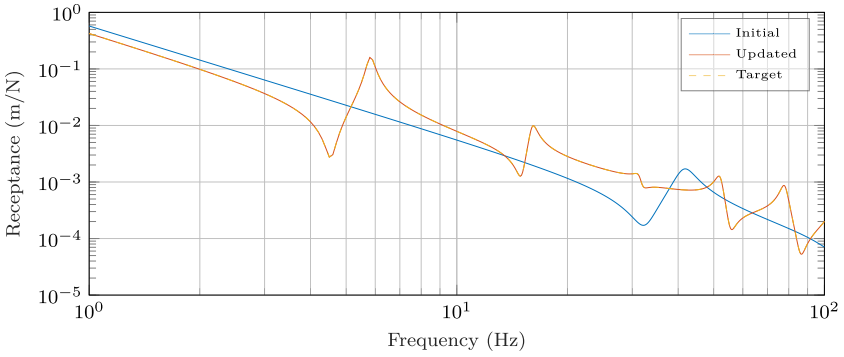

Fig. 10. Initial, updated and target transfer receptance $Y_{lc_{11}c_{21}}$. Note that the updated and target curves are near indistinguishable.

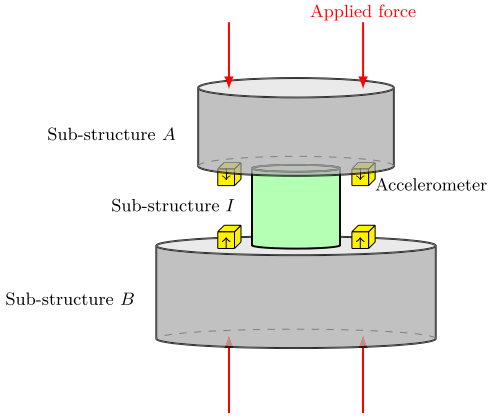

Fig. 11. Characterisation assembly *AIB* for the vibration isolator transfer stiffness.

To update the sub-structure I model the following cost function is defined,

$$J(\theta) = \sum_{\omega}^{} \sum_{a}^{} \left\| \mathbf{D}^{(FE)}_{lc_1c_2}(\omega) - \mathbf{D}^{(exp)}_{lc_1c_2}(\omega) \right\|^2 \tag{34}$$

where $\mathbf{D}^{(FE)}_{lc_1c_2}$ and $\mathbf{D}^{(exp)}_{lc_1c_2}$ are the transfer stiffness matrices from the uncoupled (to be updated) and coupled (test) sub-structure models. Eq. (34) is then minimised using a gradient based optimisation with N random initialisations.

Shown in Fig. 10 are the target and updated transfer receptances $Y_{lc_{11}c_{21}}$. Also shown is an example of an initial transfer receptance from which the updating procedure began. As expected given the numerical nature of this example, the updated sub-structure model is in agreement with the target sub-structure. Importantly, this updating procedure was based entirely on *coupled assembly simulations*, yet it was able to refine a model of sub-structure I alone.

5. Experimental case study: Dynamic sub-structuring with in-situ updated FE isolator models

The experimental case study presented in this section demonstrates a practical application of in-situ model updating using a relatively simple but realistic sub-structure. The sub-structure considered is a cylindrical rubber vibration isolator (see Fig. 13).

Vibration isolators, among other resilient couplings, provide a notable application of the in-situ updating approach. Unlike typical sub-structures, the characteristics of vibration isolators are sensitive to pre-load, among other installation conditions, so can only be characterised whilst installed within an assembly (e.g. a test rig). A conventional model updating would require either: a) the isolator to be physically constrained or b) the test rig to be included as part of the model to be updated. The in-situ approach avoids this entirely, requiring only in-situ measurements and a model of the isolator.

The aim of this example is to update the numerical model of a vibration isolator, based on in-situ experimental data and sub-structure invariants (dynamic transfer stiffness). The assembly used for model updating consists of a rigid mass coupled either side of a single isolator, as shown in Fig. 11. To verify that the updated isolator model is representative of the physical element, it is used to predict the response of a complex built-up structure. This form of validation is necessary to avoid the unrepresentative boundary conditions obtained when the isolator is removed from its assembly, as required for an independent validation.

Please cite this article as: J.W.R. Meggitt and A.T. Moorhouse, Finite element model updating using in-situ experimental data, Journal of Sound and Vibration, https://doi.org/10.1016/j.jsv.2020.115675

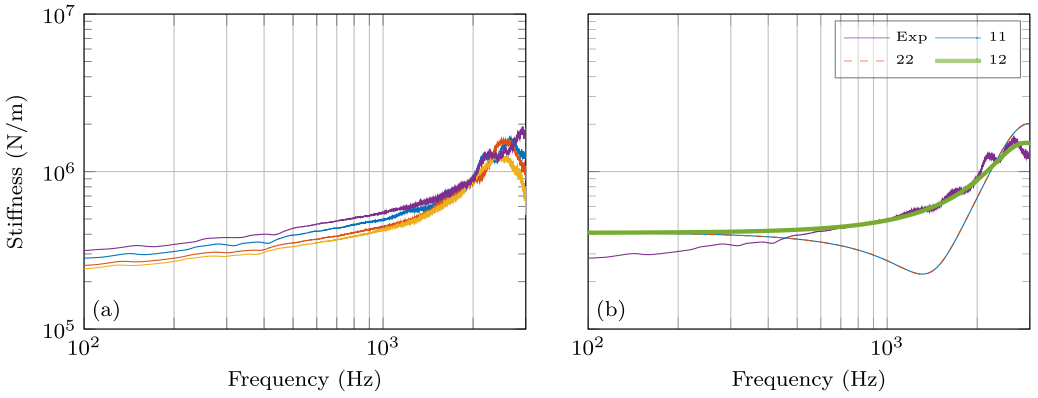

Fig. 12. In-situ model updating of a vibration isolator. (a) - experimental dynamic transfer stiffness of all four isolators considered. (b) - an example of the in-situ updated FE point and transfer stiffness based on a single isolator, where: 11 is the point stiffness at interface c_1, 22 is the point stiffness at interface c_2, and 12 is the transfer stiffness between interface c_1 and c_2. (For interpretation of the references to colour in this figure legend, the reader is referred to the web version of this article.)

The validation assembly considered is shown in Fig. 13, and consists of a 4-footed motor (source, S) coupled to a large aluminium plate (receiver, R) via 4 vibration isolators. Note that the proposed in-situ updating strategy is applied to each isolator independently. The assembly's receptance matrix is obtained using a primal dynamic sub-structuring (DS) prediction consisting of: experimental source and receiver receptences, and an updated FE model of each vibration isolator. Results are compared against receptances obtained directly from the coupled assembly.

In summary, the steps followed were:

1) Measure the interface receptance matrix $\mathbf{Y}_{AIB}$ of each vibration isolator whilst installed in a secondary assembly (see Fig. 11), and extract their dynamic transfer stiffness (sub-structure invariant) by matrix inversion, as per Eq. (27).
2) Construct a simplified FE rod model for each vibration isolator and update to minimise a proposed cost function.
3) Use updated FE model to obtain isolator receptance matrix $\mathbf{Y}_I^{FE}$. Note that sub-structures A and B are not included in the updated FE model; only the isolator sub-structure is modelled.
4) Characterise source and receiver sub-structures (see Fig. 13) experimentally by their free interface receptance matrices, $\mathbf{Y}_S^{\text{exp}}$ and $\mathbf{Y}_R^{\text{exp}}$.
5) Use DS to assemble $\mathbf{Y}_S^{\text{exp}}$, $\mathbf{Y}_I^{FE}$ and $\mathbf{Y}_R^{\text{exp}}$, thus forming the coupled receptance $\mathbf{Y}_{SIR}^{hyb}$ (representing the validation assembly in Fig. 13), where *hyb* is used to denote a '*hybrid*' assembly prediction (hybrid indicates that it combines modelled isolator properties with measured receptances of the other two sub-structures).
6) Compare the hybrid receptance prediction $\mathbf{Y}_{SIR}^{hyb}$ against to those obtained directly from the coupled assembly $\mathbf{Y}_{SIR}^{\text{exp}}$.

5.1. Element characterisation

Each vibration isolator was characterised using the in-situ matrix inversion approach described in Section 2.2. Characterisation was performed using a mass-isolator-mass assembly, as shown diagrammatically in Fig. 11. Note that rigid masses were used as connected sub-structures but the method is not restricted to such elements and can also be performed in the presence of resonant connected sub-structures [14]. A pair of spaced accelerometers were adhered to the upper and lower interface, c_1 and c_2, and a force applied at each. Appropriate averaging yielded the interface receptance matrix $\mathbf{Y}_{AIB}$, from which the transfer stiffness was obtained by inversion, as per Eq. (27).

Shown in Fig. 12a are the transfer stiffnesses of each vibration isolator. These stiffness values are used to update an FE model of each vibration isolator.

5.2. Finite element model

The vibration isolators used in this example were solid, cylindrical, rubber type elements and were modelled with a simplified FE model using basic rod elements with viscous damping.

The isolator dynamic stiffness matrix is given by

$$\mathbf{D} = \mathbf{K} - \omega^2\mathbf{M} \tag{35}$$

where $\mathbf{M}$ and $\mathbf{K}$ are the assembled mass and stiffness matrices of the rod element, and ω is the evaluated frequency. Note that the stiffness matrix $\mathbf{D}$ must be dynamically reduced to the interface DoFs c_1 and c_2 if it is to be evaluated against an experimental transfer stiffness.

To simplify the updating procedure, only global element properties were set as updating parameters (i.e. it was assumed that the element's properties did not vary across its length). The length, cross sectional area, Young's modulus, density and

Please cite this article as: J.W.R. Meggitt and A.T. Moorhouse, Finite element model updating using in-situ experimental data, Journal of Sound and Vibration, https://doi.org/10.1016/j.jsv.2020.115675

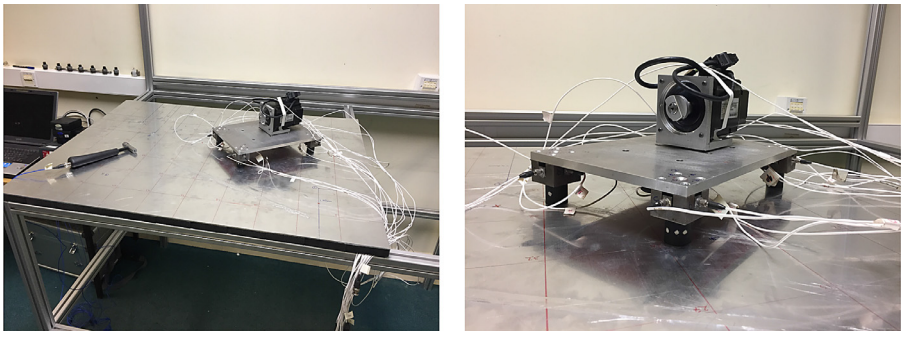

Fig. 13. Photos of experimental the validation assembly. Left - coupled assembly. Right - source sub-structure.

damping coefficient were set as updating parameters, $\theta = (I, S, E, \rho, \eta)$, and used to minimise the cost function,

$$J_D(\theta) = \sum_{\omega} \left| \tilde{D}^{FE}_{lc_1c_2}(\theta) - D^{exp}_{lc_1c_2} \right|^2 + \sum_{n} |\Delta\omega|^2_n \tag{36}$$

where, $D^{\text{exp}}_{lc_1c_2}$ is the dynamic transfer stiffness obtained from experiment (shown in Fig. 12a for the four isolators), $\tilde{D}^{FE}_{lc_1c_2}$ is the reduced transfer stiffness obtained from the FE model, and $|\Delta\omega|_n$ is the frequency difference between the nth FE and experimental stiffness peak. A MATLAB implementation of the simplex search method [26] (*fminsearch( )*) was used to minimise Eq. (36).

Shown in Fig. 12b are the updated FE stiffness values for a single isolator. In purple is the experimental transfer stiffness used in the updating procedure, and in green is the updated transfer stiffness obtained from the FE model. Also shown in blue and orange are the point stiffness values of the FE isolator model. Note that the point stiffness is not available by matrix inversion; its characterisation requires a more complex sub-structure decoupling procedure [27]. The proposed in-situ updating therefore has the potential to provide a convenient means of determining the point stiffness of a vibration isolator from in-situ measurements alone. This is a noteworthy application of in-situ updating, as not being able to obtain an isolator's point stiffness can be a limiting factor in the prediction of high frequency vibration in assembled structures.

As expected given its simplicity, good agreement is obtained between the experimental and numerical transfer stiffness across the frequency range considered, particularly in the vicinity of the internal mount resonance (1–3 kHz). Note that there is some disagreement in the low-mid frequency trend ($\approx$ 100-500 Hz) between the experimental and numerical transfer stiffnesses. This is likely a result of some minor frequency dependence in the material properties of the element that is not accounted for by the simplified FE model.

5.3. Sub-structuring results

Having obtained an updated FE model for each isolator we're able to perform a DS prediction of the coupled assembly (see Fig. 13) for the purpose of validating the numerical model. Using a primal DS formulation [28] the coupled assembly receptance matrix $\mathbf{Y}_{SIR} \in \mathbb{C}^{9\times9}$ is given by,

$$\mathbf{Y}_{SIR} = \left(\mathbf{L}^{\mathrm{T}}[\mathbf{D}]\mathbf{L}\right)^{-1} \tag{37}$$

where $[\mathbf{D}] \in \mathbb{C}^{17\times17}$ is the block diagonal sub-structure stiffness matrix, given by,

$$[\mathbf{D}] = \begin{bmatrix} \mathbf{Y}^{\text{exp}}_{S} & & & & & & \\ & \mathbf{Y}^{FE}_{I_{(1)}} & & & & & \\ & & \mathbf{Y}^{FE}_{I_{(2)}} & & & & \\ & & & \mathbf{Y}^{FE}_{I_{(3)}} & & & \\ & & & & \mathbf{Y}^{FE}_{I_{(4)}} & & \\ & & & & & \mathbf{Y}^{\text{exp}}_{R} \end{bmatrix}^{-1} \tag{38}$$

and $\mathbf{L} \in \mathbb{Z}^{17\times9}$ is a Boolean coupling matrix that enforces compatibility and equilibrium constraints between appropriate interface DoFs. The free interface source and receiver receptance are given, respectively, by $\mathbf{Y}^{\text{exp}}_{S} \in \mathbb{C}^{4\times4}$ and $\mathbf{Y}^{\text{exp}}_{R} \in \mathbb{C}^{5\times5}$, and the ith isolator receptance matrix by $\mathbf{Y}^{FE}_{I_{(i)}} \in \mathbb{C}^{2\times2}$.

Shown in Fig. 14 are the directly measured (blue) and predicted (orange) transfer receptances between each foot of the source and a remote receiver DoF in the coupled assembly. Good agreement is obtained in all cases, demonstrating that the in-situ updated models correctly describe the dynamics of the vibration isolators.

It is worth noting that without the aid of the updated FE models the above prediction would be limited by the requirement that $D_{lc_1c_1} \approx -D_{lc_1c_2}$, i.e. that the vibration isolators behave as ideal springs [29]. From Fig. 12b it is clear that this true

Please cite this article as: J.W.R. Meggitt and A.T. Moorhouse, Finite element model updating using in-situ experimental data, Journal of Sound and Vibration, https://doi.org/10.1016/j.jsv.2020.115675

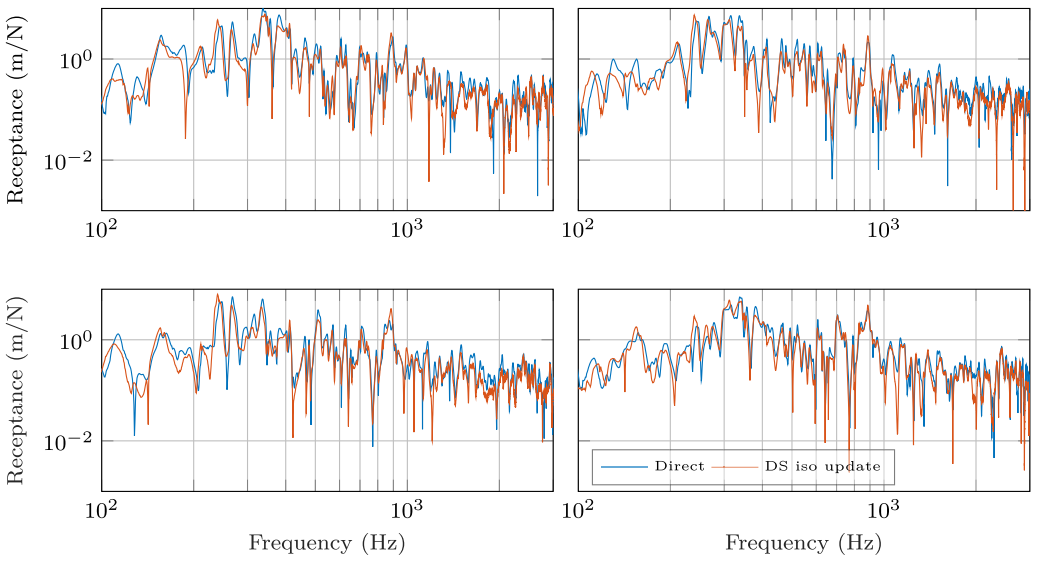

Fig. 14. Transfer receptance between each source foot and remote receiver DoF for the directly measured assembly (in blue) and DS prediction using an in-situ updated FE isolator model. (For interpretation of the references to colour in this figure legend, the reader is referred to the web version of this article.)

only in the low frequency range, below approx. 400 – 500 Hz. This application of in-situ model updating thus provides a convenient means of a) characterising vibration isolators and b) extending the predictive range of high frequency vibration in resiliently coupled structures.

6. Conclusions

The purpose of this paper has been to propose and verify the application of *in-situ* experimental testing as a means of updating numerical *sub-structure* models. Conventional model updating requires the target sub-structure to be uncoupled and freely suspended, thus enabling the direct measurement of its invariant properties, such as its free interface receptance. Achieving this idealised boundary condition however, is often impractical. Furthermore, it is in conflict with the requirement that the sub-structure should also be under a representative loading; this is particularly so when considering coupling elements such as vibration isolators.

By exploiting recent advances regarding the in-situ characterisation of sub-structures, it has been shown that it is possible to extract invariant sub-structural properties from measurements performed on the *assembly* in which the target sub-structure is installed, thus avoiding the need for free suspension. The extraction of such invariant properties is made possible by the constraints present in their definitions. By placing these constraints at the sub-structure interface it is possible to mathematically enforce a rigid constraint, thus removing the effect of any unknown boundary conditions (i.e. the influence of neighbouring sub-structures).

Sub-structural invariants include the force and displacement transmissibility and the dynamic transfer and point stiffness. Whilst a detailed investigation of various possible forms of optimisation procedure was not part of this study, good results were obtained using established algorithms and simple cost functions. It was also discussed how established transmissibility-based updating methods [11,12] can be applied with far greater flexibility than originally envisaged, specifically to the problem of updating a sub-structure model whilst it is embedded within an assembly.

The proposed in-situ updating strategy was illustrated through a numerical example, considering FE beam structures. A practical example was also shown in which an FE model of a vibration isolator was developed and updated against a physical isolator without it being removed from an assembly. It was shown that by using the updated isolator model(s) a DS prediction could be made for a resiliently coupled assembly over a wide frequency range; notably up to 3kHz.

Declaration of Competing Interest

The authors declare that they have no known competing financial interests or personal relationships that could have appeared to influence the work reported in this paper.

CRediT authorship contribution statement

J.W.R. Meggitt: Conceptualization, Methodology, Validation, Investigation, Writing - original draft, Writing - review & editing. **A.T. Moorhouse:** Writing - review & editing.

Please cite this article as: J.W.R. Meggitt and A.T. Moorhouse, Finite element model updating using in-situ experimental data, Journal of Sound and Vibration, https://doi.org/10.1016/j.jsv.2020.115675

References

[1] J.E. Mottershead, M.I. Friswell, Model updating in structural dynamics: a survey, 1993. doi:10.1006/jsvi.1993.1340.
[2] M.I. Friswell, J.E. Mottershead, Finite element model updating in structural dynamics, 38, 1995, doi:10.1007/978-94-015-8508-8.
[3] G. Steenackers, P. Guillaume, Finite element model updating taking into account the uncertainty on the modal parameters estimates, J. Sound Vib. 296 (4–5) (2006) 919–934, doi:10.1016/j.jsv.2006.03.023.
[4] R.M. Lin, D.J. Ewins, Analytical model improvement using frequency response functions, Mech. Syst. Signal Process. 8 (4) (1994) 437–458, doi:10.1006/mssp.1994.1032.
[5] M. Imregun, W.J. Visser, D.J. Ewins, Finite element model updating using frequency response function data I. theory and initial investigation, Mech. Syst. Signal Process. 9 (2) (1995) 187–202, doi:10.1006/mssp.1995.0015.
[6] M. Imregun, K.Y. Sanliturk, D.J. Ewins, Finite element model updating using frequency response function data II. Case study on a medium-size finite element model, Mech. Syst. Signal Process. 9 (2) (1995) 203–213, doi:10.1006/mssp.1995.0016.
[7] K.J. Chang, Y.P. Park, Substructural dynamic modification using component receptance sensitivity, Mech. Syst. Signal Process. 12 (4) (1998) 525–541, doi:10.1006/mssp.1998.0184.
[8] K.S. Kwon, R.M. Lin, Frequency selection method for FRF-based model updating, J. Sound Vib. 278 (1–2) (2004) 285–306, doi:10.1016/j.jsv.2003.10.003.
[9] J.E. Mottershead, On the zeros of structural frequency response functions and their application to model assessment and updating, Proc. Int. Modal Anal. Conf. - IMAC 1 (1998) 500–503.
[10] C. Devriendt, P. Guillaume, The use of transmissibility measurements in output-only modal analysis, Mech. Syst. Signal Process. 21 (7) (2007) 2689–2696, doi:10.1016/j.ymssp.2007.02.008.
[11] G. Steenackers, C. Devriendt, P. Guillaume, On the use of transmissibility measurements for finite element model updating, J. Sound Vib. 303 (3–5) (2007) 707–722, doi:10.1016/j.jsv.2007.01.030.
[12] V. Meruane, Model updating using antiresonant frequencies identified from transmissibility functions, J. Sound Vib. 332 (4) (2013) 807–820, doi:10.1016/j.jsv.2012.10.021.
[13] A.T. Moorhouse, A.S. Elliott, T.A. Evans, In situ measurement of the blocked force of structure-borne sound sources, J. Sound Vib. 325 (4–5) (2009) 679–685, doi:10.1016/j.jsv.2009.04.035.
[14] J.W.R. Meggitt, On In-situ Methodologies for the Characterisation and Simulation of Vibro-Acoustic Assemblies, University of Salford, 2017 Phd.
[15] J.W.R. Meggitt, A.S. Elliott, A.T. Moorhouse, In-situ determination of dynamic stiffness for resilient elements, J. Mech. Eng. Sci. 230 (6) (2015) 986–993, doi:10.1177/0954406215618986.
[16] N.M.M. Maia, a. P. V. U. Urgueira, R. a. B., R.a.B Almeida, Whys and Wherefores of Transmissibility(2011) 352. doi:10.5772/24869.
[17] Y.E. Lage, M.M. Neves, N.M.M. Maia, D. Tcherniak, Force transmissibility versus displacement transmissibility, J. Sound Vib. 333 (22) (2014) 5708–5722, doi:10.1016/j.jsv.2014.05.038.
[18] J.W.R. Meggitt, A.T. Moorhouse, A.S. Elliott, On the problem of describing the coupling interface between substructures: an experimental test for completeness', in: Proceedings of the 36th International Modal Analysis Conference - IMAC, 4, Conference Proceedings of the Society for Experimental Mechanics Series, 2018, pp. 1–12.
[19] J.W.R. Meggitt, A.T. Moorhouse, On the completeness of an interface description and the consistency of blocked forces obtained in-situ, Mech. Syst. Signal. Process. 145 (106850) (2020).
[20] Y.I. Bobrovnitskii, A theorem on the representation of the field of forced vibrations of a composite elastic system, Acoust. Phys. 47 (5) (2001) 586–589.
[21] A.M.R. Ribeiro, J.M.M. Silva, N.M.M. Maia, On the generalisation of the transmissibility concept, Mech. Syst. Signal Process. 14 (1) (1998) 29–35, doi:10.1006/mssp.1999.1268.
[22] P. Gajdatsy, K. Janssens, W. Desmet, H. Van Der Auweraer, Application of the transmissibility concept in transfer path analysis, Mech. Syst. Signal Process. 24 (7) (2010) 1963–1976, doi:10.1016/j.ymssp.2010.05.008.
[23] M. Haeussler, S.W.B. Klaassen, D.J. Rixen, Comparison of Substructuring based techniques for dynamic property identification of rubber isolators, in: ISMA 2018 - International Conference on Noise and Vibration Engineering, August, 2018, p. 1.
[24] J.W.R. Meggitt, A.T. Moorhouse, In-situ sub-structure decoupling of resiliently coupled assemblies, Mech. Syst. Signal Process. 117 (2019) 723–737, doi:10.1016/j.ymssp.2018.07.045.
[25] V. Meruane, W. Heylen, Structural damage assessment with antiresonances versus mode shapes using parallel genetic algorithms, Struct. Control Health Monitor. (May 2011) (2011), doi:10.1002/stc.
[26] J.C. Lagarias, A.A. Reeds, M.H. Wright, P.E. Wright, Convergence properties of the nelder-Mead simplex method in low dimensions, Siam J. Optim. 9 (1) (1998) 112–147.
[27] M. Haeussler, S.W.B. Klaassen, D.J. Rixen, Experimental twelve degree of freedom rubber isolator models for use in substructuring assemblies, J. Sound Vib. 474 (2020) 9–11, doi:10.1016/j.jsv.2020.115253.
[28] D. de Klerk, D.J. Rixen, S.N. Voormeeren, General framework for dynamic substructuring: history, review and classification of techniques, AIAA J. 46 (5) (2008) 1169–1181, doi:10.2514/1.33274.
[29] J.W.R. Meggitt, A.S. Elliott, A.T. Moorhouse, Virtual assemblies and their use in the prediction of vibro-acoustic responses, in: Proceedings of the Institute of Acoustics, 2016. Warickshire.

Please cite this article as: J.W.R. Meggitt and A.T. Moorhouse, Finite element model updating using in-situ experimental data, Journal of Sound and Vibration, https://doi.org/10.1016/j.jsv.2020.115675